Journal of Hydroscience and Hydraulic Engineering
Vol. 11, No. 1, May, 1993, 67-77

NUMERICAL SIMULATION OF A VACUUM PERMEABILITY TEST IN HETEROGENEOUS GROUND

By

Takeshi Kawatani

Institute of Reclamation Engineering, Faculty of Engineering,
Kobe University, Kobe 657, Japan

Akihiko Nakayama

Institute of Reclamation Engineering, Faculty of Engineering,
Kobe University, Kobe 657, Japan

and

Shunji Ikemiya

Division of Engineering, Graduate School, Kobe University
Kobe 657, Japan

SYNOPSIS

The intrinsic permeability may be a useful index for determining the excavation-damaged, loosened zones in fissured and fractured rock mass. Jakubick and Klein performed a vacuum borehole logging test in dry rock and deduced the permeability employing methods based on the equations for two-dimensional, axisymmetric gas flows in an isotropic, homogeneous porous medium. However, the flow induced by the test is considered quite different from the one assumed in their data analysis.

Numerical simulations are carried out herein to know how the pressure recovery in a borehole test section is affected by the extent and degree of the loosened zone, and what the derived permeabilities represent. In addition, an inverse analysis is performed to determine the permeabilities from the pressure-recovery data obtained in the aforementioned simulations.

The results indicate the following: a) the extent of the loosened zone can be infered from the pressure and the rate of its recovery at the late stage of the test; b) the degree of looseness can be estimated from the rate of pressure recovery at the early stage as well as from the flow rate during the pumping phase; and c) the permeability determined by the inverse analysis seems to represent the permeability of the vicinity of test section.

INTRODUCTION

Large-scale excavations in a rock mass cause the enlargement of interstices in the fissured and fractured zones because of the vibrations during excavations and stress relaxation. As a result, the permeability becomes larger in the excavation-loosened zone around the cavern compared to deeper zones. Hence, the permeability can be a measure of the degree and the extent of the loosened zone. Jakubick and Klein(4) carried out a vacuum borehole logging test to determine the excavation-damaged zone from the permeability distribution along a borehole. The procedure of this test follows closely the standard pressure buildup testing procedure used in the petroleum industry. For the estimation of permeability from the raw data of

pressure in the test section and the air flow rate, Jakubick and Klein(3) employed the relationships for two-dimensional axisymmetric air-flow in an isotropic homogeneous porous medium. The actual flow induced in rocks during the test, however, is considered quite different from the flow mentioned above. Since the openings are larger in the loosened zone around the cavern than in deeper zones, it is expected that the air flowing into the test section is supplied mostly through the excavation surface. This means that the flow field is three-dimensional and heterogeneous. Therefore, it is important to know prior to the data analyses how the pressure-recovery process is affected by the extent of the loosened zone and the position of test section, and what the evaluated permeabilities represent. The objective of this numerical study is to clarify the above points. The simulation is performed employing a Galerkin finite element method and solving the governing equations for three-dimensional axisymmetric gas-flow.

An inverse analysis is also performed to examine its applicability to the data analysis. In the inverse analysis, the pressure recoveries obtained in the simulation are taken as inputs assuming the porous medium to be homogeneous, and the permeabilities which reproduce the input are determined.

MODELING

Before setting up a model for the simulation, the test performed by Jakubick and Klein(4) is described in the following. The vacuum permeability measurements were performed in dry rocks. The boreholes were drilled nearly at right angle to the excavation surface. They were 6m long and 37.7mm in diameter. Both ends of the test section were sealed by packers. The test section was 25cm long, although the length is adjustable from 10 to 50cm by the sealing equipment. Using a vacuum pump, the air in the test section was evacuated until both pressure and flow conditions were stabilized. The pump was then shut off to initiate the pressure recovery process. Throughout the pumping and the recovery phases, the pressure in the test section was measured together with the ambient pressure and temperature. The air-flow rate was also monitored during the pumping phase. The permeability distribution along the borehole was obtained by moving the test section and performing the measurement repeatedly.

As mentioned above, Jakubick and Klein(3) assumed in the data analysis that the flow was a two dimensional, radial flow in a homogeneous formation of infinite horizontal extent. It is deduced from their assumption that the rock formation consists of layers perpendicular to the borehole axis each of which is 25cm thick and the flow in a certain layer is independent of those in other layers. In fact, as shown schematically in Fig.1, the air flowing into the test section is considered to enter the interstices of rock mass mainly through the excavation surface. Taking these points into account, the following model is employed.

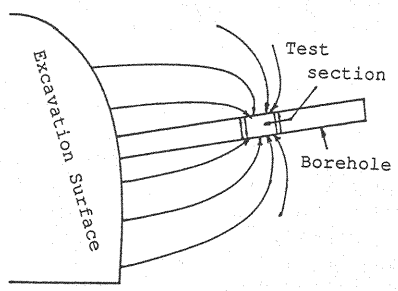

Fig. 1 Schematic flow induced by a permeability test.

The density of interstices is assumed to be so high that the fractured rock is regarded as a porous medium. Air enters the openings only from the excavation surface. The flow field is symmetric with respect to the borehole axis which is perpendicular to the excavation surface. Namely, the flow region is a cylinder whose axis coincides with the borehole axis. One end of the cylinder corresponds to the excavation surface. The flow region is 7m long and 10m in diameter. The diameter of the borehole is 4cm. The test section is 25cm long.

METHOD OF SIMULATION

The continuity equation for axisymmetric seepage flows is

$$\phi\frac{\partial \rho}{\partial t} + \frac{1}{r}\frac{\partial}{\partial r}(r\rho q_r) + \frac{\partial}{\partial z}(\rho q_z) = 0 \qquad (1)$$

where t is the time, z and r are the longitudinal and radial coordinates, respectively, ρ is the density of the air, q_r and q_z are the apparent velocities in the r- and z-directions and ϕ is the porosity.

When Darcy's law is applicable and the coordinates coincide with the principal axes of the permeability tensor, the apparent velocities are given by

$$q_r = -\frac{k_r}{\mu}\frac{\partial p}{\partial r}, \qquad q_z = -\frac{k_z}{\mu}\frac{\partial p}{\partial z} \tag{2}$$

where p is the air pressure, k_r and k_z are the intrinsic permeabilities in the r- and z-directions and μ is the viscosity of the air.

The equation of state for an ideal gas is applicable to the air with sufficient accuracy(6). Thus, $\rho = p/RT$ where T is the temperature, and R stands for the gas constant for air. In a special case in which the thermodynamic process is adiabatic, the equation of state is written as $p/\rho^{\kappa} = \text{const}$ where $\kappa = c_p/c_v$, c_p and c_v are the specific heat capacities at constant pressure and at constant volume, respectively. κ=1.40 for dry air. Hence, for both isothermal and adiabatic processes, the equation of state can be written as

$$\rho = Cp^{\eta} \tag{3}$$

where η =1.0 (for isothermal process) or 1/1.4 (for adiabatic process), and C is a constant.

The equation is obtained from Eqs.1, 2 and 3 as follows,

$$\phi\eta r\frac{1}{p}\frac{\partial \Psi}{\partial t} - \frac{\partial}{\partial r}\left(r\frac{k_r}{\mu}\frac{\partial \Psi}{\partial r}\right) - \frac{\partial}{\partial z}\left(r\frac{k_z}{\mu}\frac{\partial \Psi}{\partial z}\right) = 0 \tag{4}$$

where $\Psi = p^{1+\eta}$.

The pressure in the test section during the recovery phase is calculated by following processes. The equation for mass conservation in the test section is written as

$$V_B\frac{\partial \rho_B(t)}{\partial t} = M_B \tag{5}$$

where $\rho_B(t)$ is the density of the air in the test section at t, V_B denotes the volume of the test section, and M_B is the mass flux into the test section given by

$$M_B = -2\pi r_B\int_{z_B}\rho q_r|_{r=r_B}\,dz = 2\pi r_B\int_{z_B}\frac{Ck_r}{(\eta+1)\mu}\frac{\partial \psi}{\partial r}|_{r=r_B}\,dz$$

in which r_B and z_B denote the radius and length of the test section, respectively. Then, the finite difference approximation of Eq.5 is $\rho_B(t+\Delta t) = \rho_B(t) + M_B\Delta t/V_B$ where Δt is the time increment. Thus, in a case of isothermal or adiabatic process, the pressure in the section at $t+\Delta t$ is

$$p_B(t+\Delta t) = \{\rho_B(t+\Delta t)/\rho_0\}^{1/\eta}p_0 \tag{6}$$

where p_B is the pressure in the test section, p_0 is the atmospheric pressure(1 atm), and ρ_0 is the density of the air at p_0.

The discretization of Eq.4 by means of a Galerkin finite element method yields

$$[A]\left\{\frac{d\psi}{dt}\right\} + [B]\{\psi\} = \{D\} \tag{7}$$

where the elements of the matrices [A] and [B], and the column vector {D} are

$$A_{nm} = \Sigma \int_{Re} \alpha_p I_n I_m dR$$

$$B_{nm} = \Sigma \int_{Re} \left(r \frac{k_r}{\mu} \frac{\partial I_n}{\partial r} \frac{\partial I_m}{\partial r} + r \frac{k_z}{\mu} \frac{\partial I_n}{\partial z} \frac{\partial I_m}{\partial z} \right) dR$$

$$D_n = - \Sigma \int_{se} Q_B I_n ds$$

and $\alpha_p = \rho \eta r / p$. Here, I_n stands for an interpolation function, R_e and S_e are the flow region and its boundary, respectively, and Σ denotes the summation over all elements. Also, Q_B is the prescribed flux across the boundary of the flow region and is given by

$$Q_B = - \left(r \frac{k_r}{\mu} \frac{\partial \psi}{\partial r} n_r + r \frac{k_z}{\mu} \frac{\partial \psi}{\partial z} n_z \right)$$

Replacement of the time derivative in Eq.7 by a three-time-level finite difference approximation(2) yields

$$[E]\{ \psi^{(t+\Delta t)} \} = \{ F \} \tag{8}$$

where the elements of the matrix [E] and the column vector {F} are given by

$$E_{nm} = \frac{3}{2\Delta t} A_{nm}^{(t)} + B_{nm}$$

$$F_n = - B_{nm} \psi_m^{(t)} + \left(\frac{3}{2\Delta t} A_{nm}^{(t)} - B_{nm} \right) \psi^{(t-\Delta t)} + 3 D_n^{(t)}$$

and superscript(t) means the values at time t. The numerical solution of Eq.7 is unconditionally stable. On the other hand, a forward finite difference approximation of the same equation gives

$$[E']\{ \psi^{t+\Delta t} \} = \{ F' \} \tag{9}$$

where the elements of the matrix [E'] and the column vector {F'} are given by

$$E'_{nm} = A_{nm}^{(t)}$$

$$F'_n = \left(A_{nm}^{(t)} - \Delta t D_n^{(t)} \right) \psi_m^{(t)} + \Delta t D_n^{(t)}$$

Treating the medium as homogeneous, an inverse analysis is performed to determine the permeabilities which reproduce the pressure-recovery processes obtained in the forward analyses described above as close as possible. A constrained simplex method(1,5) is used for the inverse analysis in which the objective function is defined by

$$f_j = \sum_{i=1}^{N} \left\{ \frac{p_i - p^*_i}{p_i} \right\}_j^2 \tag{10}$$

where f_j is the objective function evaluated at the j-th vertex of a simplex, p_i and p_i^* are the test-section pressures at the time-level i obtained by the forward and the inverse analyses, respectively, and N stands for the number of the pressure data.

SIMULATION CONDITIONS

The flow region is, as explained before, 7m deep and 10m in diameter. The air pressure on the excavation surface is fixed at 1 atm, and the initial pressure in the entire flow region is 1 atm as well. The pressure in the test section is instantaneously reduced to 0.1 atm and kept at 0.1 atm during the pumping phase. On the other hand, during recovery phase, the pressure in the test section calculated by Eq.6 is employed as the prescribed pressure on the test-section wall. All boundaries except the excavation surface and the test section are impermeable.

The intrinsic permeability of the undamaged rock mass is assumed to be $10^{-11}cm^2$. The permeability in the excavation-damaged zone is assumed to be three times as large as that in the undamaged zone. The extent of the loosened zones studied here is listed in Table 1. The viscosity of air is $1.84x1^{-5}Pa \cdot s$. The porosity is 0.1 regardless of the looseness. Assuming the process to be isothermal, the value of η in Eq.6 is 1.0.

Table 1 Extent of loosened zone

Case	Extent of loosened zone
C0	none
C1	$z \leq 2.75m$
C2	$z \leq 3.00m$
C3	$z \leq 3.50m$
C4	entire region
C5	$2.50m \leq z \leq 3.75m$ and $r \leq 0.5m$

The flow region is divided into quadrilateral elements. The number of the elements is 680 and that of the nodes is 738. The largest element is 50cm(Δr) x 25cm(Δz) while the smallest is 2cm(Δr) x 5cm(Δz). The time increment Δt is 10 seconds.

Preliminary calculations were performed to examine the effects of the size of the excavation surface. The pressure recoveries were calculated in the cases where the excavation surfaces were circles of diameter 7m and 10 m, respectively. The area of the former is about one half of the latter. The difference between the two was found to be sufficiently small. The effect of the distance between the test section and the excavation surface was also investigated. The pressure recoveries in the cases where the test section was z=3 to 3.25m and z=6 to 6.25m were quite similar to each other. Hence, in the following simulations, the diameter of the excavation surface is fixed at 10m and the test section is located at z=3 to 3.25 cm.

The pressure-recovery curves used in the inverse analysis are those obtained after the flow attained a steady state. The objective functions are evaluated at 30 seconds, 1,2,3,4 and 5 minutes after the start of the pressure-recovery phase. Four vertices are taken to define a simplex. The permeabilities corresponding to the initial vertices are taken to be random numbers larger than $1.0x10^{-12}cm^2$ but smaller than $1.0x10^{-10}cm^2$. The porosity is fixed at 0.1. The search of the optimal permeability is terminated when the standard deviation of f_j becomes less than 0.001.

RESULTS

The flow rates during the pumping phase where the pressure in the test section was kept at 0.1 atm are shown in Fig.2. These results show that the flow rates are much larger in cases C3,C4 and C5 where the test section is in the loosened zone than in cases C0,C1 and C2 where the test section is in the undamaged zone. It is interesting that the flow rate in case C5 where the loosened zone is limited in a small area around the test section is almost the same as that in case C4 where the whole flow region is loosened. On the other hand, in case C2 where the loosened zone extends from the excavation surface to the top of the test section but the test section itself is in undamaged zone, the flow rate is quite similar to case C0 where there is no loosened zone. The flow rates are virtually constant by 45 minutes after the pumping is started.

The pressure distributions in the flow region 90 minutes after the pumping is started are shown in Fig.3. It can be seen that the area of the pressure depression

is larger in the loosened zone than in the undamaged zone. This can be understood as follows. Equation 4 implies that the coefficient $\lambda=kp/\rho\eta\mu$ is the diffusivity of Ψ which is larger for larger values of the intrinsic permeability k. Thus, the depression spreads faster and wider in the loosened zone.

If the pressure gradient of case C5 is compared with those of other cases, it is noticed that the gradient of case C5 is smaller in the loosened zone but larger in the undamaged zone. The pressure distributions in the loosened zones of cases C3 and C4 are quite similar, while the depression in the undamaged zone of the former case is smaller.

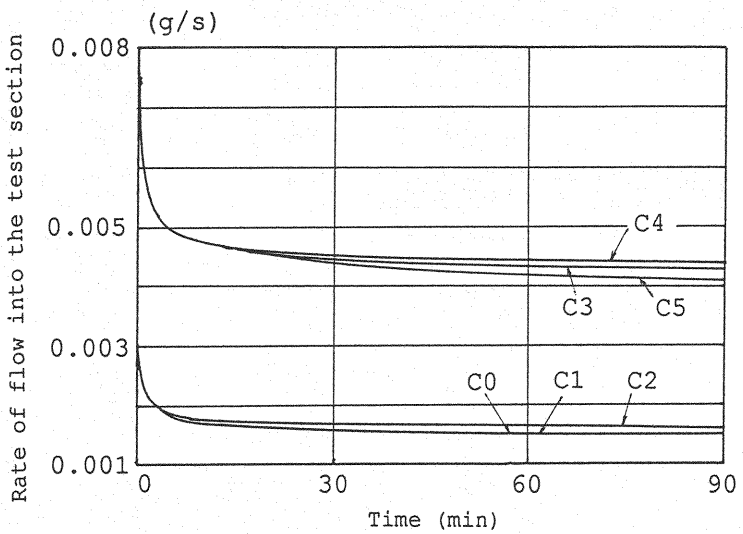

Fig. 2 Flow rates into the test section during pumping phase.

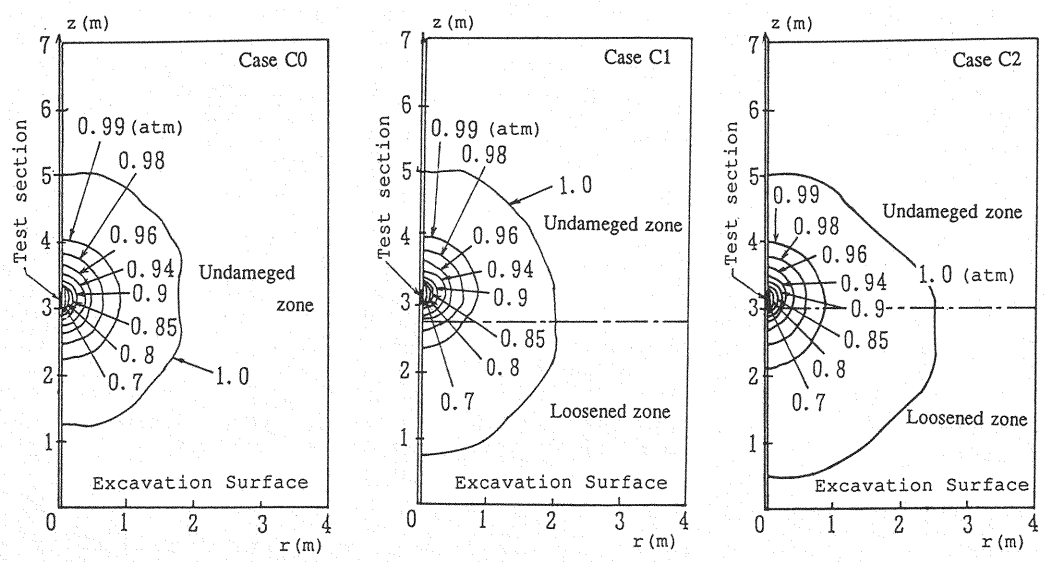

Fig. 3 (1) Pressure distributions 90 min after pumping phase started.

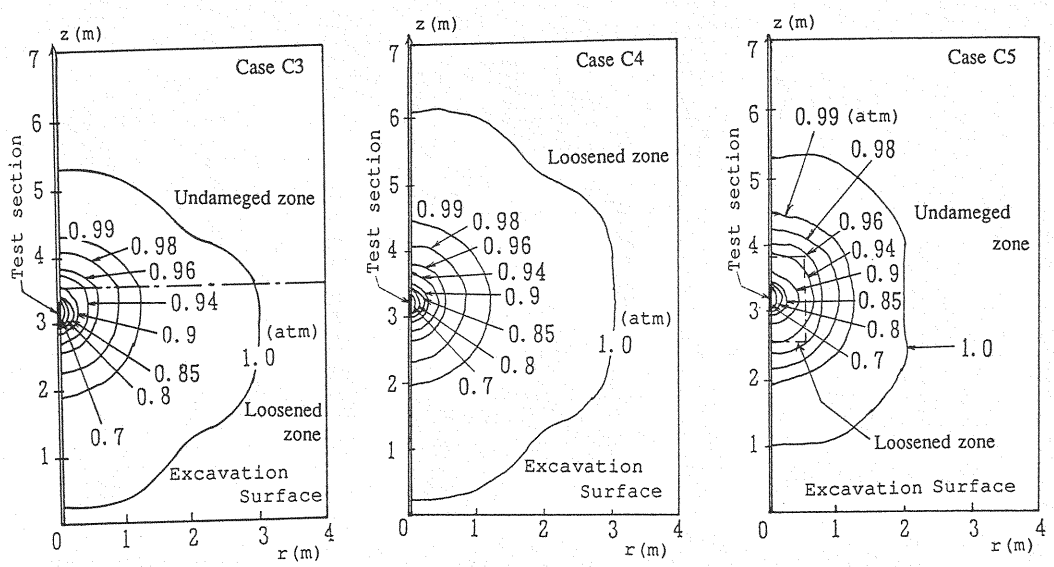

Fig. 3 (2) Pressure distributions 90 min after pumping phase started.

Figure 4 shows the pressure recoveries in the test section after a vacuum pump is activated for 30 minutes and then shut off. Figures 5 and 6 show the pressure recoveries in the cases of the pumping for 60 and 90 minutes, respectively. At the early stages of recovery, the rates of pressure-buildup in loosened zones (i.e., cases C3,C4,C5) are much faster than those in undamaged zones (i.e., cases C0,C1,C2). Therefore, it is said that the rate of pressure recovery at the early stages depends on whether or not the vicinity of the test section is loosened. The effect of the extent of loosened zone on the pressure recovery appears at the late stages and becomes more apparent as the depression zone spreads out. In Fig.6, it can be seen that the pressure recovery for case C5 becomes slower than those in cases C3 and C4 as the pressure increases. Moreover, at the late stages of recovery, the pressures in case C5 is lower than those in cases C0, C1 and C2, although in the latter cases the test section is located in the undamaged zone. The following is the reason for this.

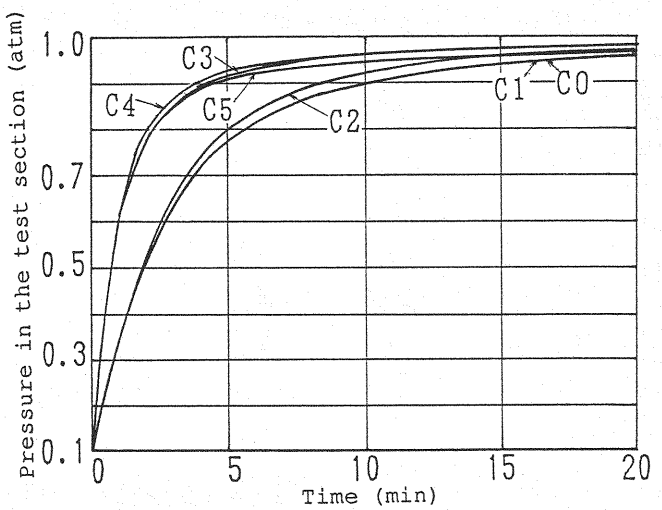

Fig. 4 Test-section pressure recoveries (pumping for 30 min before shut-off).

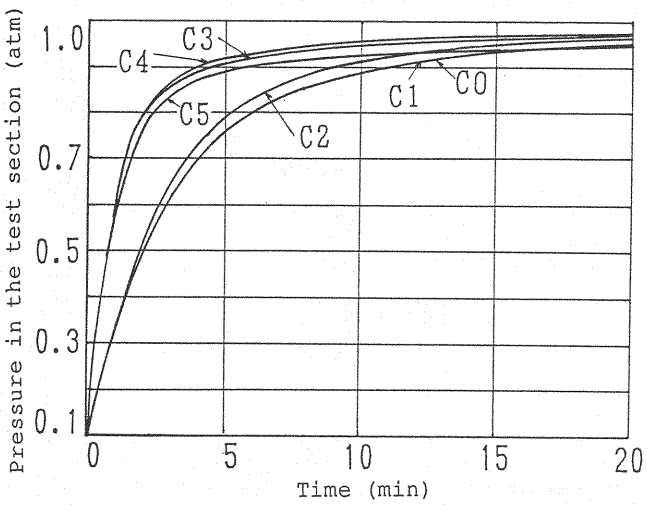

Fig. 5 Test-section pressure recoveries (pumping for 60 min before shut-off).

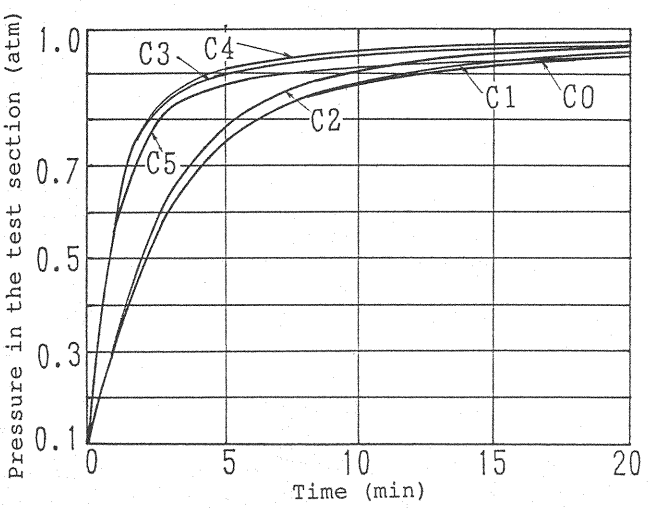

Fig. 6 Test-section pressure recoveries (pumping for 90 min before shut-off).

In order for the test-section pressure to rise, the pressure in the depression zone which surrounds the test section needs to rise as well. At the late stages of recovery, when the depression zone in which the pressure is comparable to the test-section pressure extends over a wide area, a large air supply is required to fill the test section and the pores in the depression zone. For cases C3 and C4, although the depression zones are large, the air supply is also large because of the large permeability, and the recoveries are fast. In case C5, the depression zone below 0.99 atm is the largest among all the cases studied here, and extends over the undamaged zone where the air supply is small. On the other hand, in case C2, the depression zone is smaller than that of C5, and extends over the loosened zone.

Thus, after t= 13 minutes, the pressure recovery in the test section becomes faster for case C2 than for case C5. Similar conclusion is reached in comparing cases C0 and C1 with case C5. Consequently, the extent of loosened zone around the test section can be estimated by continuing the pressure measurement until the depression zone is developed sufficiently large.

The results of the inverse analysis are given in Table 2. The deviation d_v shown in Table 2 is defined as

$$d_v = \frac{1}{N}\sum_{i=1}^{N}\frac{|p_i - p_i^*|}{p_i}$$

Table 2 Permeabilities determined by inverse analysis

Case	Calculated permeability	Deviation
C0	1.00×10^{-11} (cm^2)	0.001
C1	1.06×10^{-11} (cm^2)	0.007
C2	1.16×10^{-11} (cm^2)	0.015
C3	2.89×10^{-11} (cm^2)	0.009
C4	3.01×10^{-11} (cm^2)	0.002
C5	2.28×10^{-11} (cm^2)	0.048

In cases C0 and C4 where the entire region is homogeneous, the calculated permeabilities are practically equal to the true values. In cases C1 and C2, the calculated permeabilities are somewhat larger than the true value of undamaged zone, although both the calculated permeability and the deviation are larger in case C2 because the loosened zone extends closer to the test section. For case C3 where the loosened zone extends to the test section but the zone beyond the test section is undamaged, the calculated permeability is slightly smaller that the true value of the loosened zone. In case C5 where the loosened zone is limited in the vicinity of the test section, the calculated permeability is rather small, i.e., 76% of the true value of the loosened zone. Moreover, the deviation is considerably large compared with those in other cases.

CONCLUSIONS

A numerical simulation of a vacuum permeavility test was carried out to study how the pressure-recovery process was affected by the extent and the degree of excavation-damaged zone in the fissured and fractured rock mass. In the simulation, it was assumed that the density of the interstices in rock mass were so high that the rock was regarded as porous medium. An inverse analysis was also performed making use of the pressure-recovery curves obtained in the forward analysis. The results summarized in the following indicate that a vacuum permeability test is applicable to determine the extent and the degree of excavation-loosened zone.

1) The degree of looseness can be estimated from the rate of pressure recovery at the early stage as well as the flow rate in a stabilized state during the pumping phase.

2) The extent of loosened zone can be infered from the value to which the pressure in the test section rises asymptotically. The rate of pressure recovery at the late stages of the process is also useful in estimating the extent of the loosened zone.

3) The permeabilities, assuming the medium to be homogeneous, which reproduce the pressure-recovery curves obtained in heterogeneous media represent more or less those in the vicinity of the test section. The deviation evaluated in the inverse analysis appears useful to infer the extent of loosened zone around the test section.

REFERENCES

1. Box, M.J. : A new method of costrained optimization and a comparison with other methods, Computer Journal, Vol.8, No.1, p.425, 1965.

2. Comini, G., S.D. Guidice, R.W. Lewis and O.C. Zienkiewicz : Finite element solution of non-linear heat conduction problems with special reference to phase change, Int. J. Num. Meth. Engr., Vol.8, pp.613-624, 1974.
3. Jakubick, A.T. and R. Klein : Multiparameter testing of permeability by the transient vacuum technique: in Coupled Processes Associated with Nuclear Waste Repositories, ed. C.F. Tsang, Academic Press, pp.73-84, 1987.
4. Jakubick, A.T. and R. Klein : Permeability assessment in cavern TK-102C of underground oil storage facility in Kushikino, JAPAN, Rep. No.90-158-p, Ontario Hydro Research Division, Canada, 1990.
5. Kawatani, T., S. Nakata and S. Ikemiya : On identification of tank model parameters by a constrained simplex method, Res. Rep. of the Construction Engr. Res. Inst. Found., No.33, pp.191-204, 1991.
6. Shames, I.H. : Equation of State, Mechanics of Fluids, McGraw-Hill, New York, p.13, 1962.

APPENDIX-NOTATION

The following symbols are used in this paper:

c_p, c_v = specific heats at constant pressure and at constant volume, respectively;
d_v = deviation defined in Table 2;
f_j = objective function evaluated at the j-th vertex of a simplex;
k_r, k_z = intrinsic permeabilities in the r and z directions;
M_B = mass flux into the test section;
n_r, n_z = r- and z-components of an outer unit vector normal to the flow-region boundary;
N = number of pressure data for the inverse analysis;
p = pressure;
p_B = pressure in the test section;
p_i = test-section pressure at i-th time level obtained by the forward analysis;
p_i^* = test-section pressure at i-th time level obtained by the inverse analysis;
p_0 = atmospheric pressure;
q_r, q_z = apparennt velocities in the r and z directions, respectively;
Q_B = prescribed flux across the boundary of flow region;
r = radial coordinate of cylindrical coordinates;
r_B = radius of the test section;
R = gas constant;
R_e = area of a finite element;
S_e = boundary of a finite element which is a part of the boundary of flow region;
t = time;
Δt = time increment;
T = temperature;

V_B = volume of the test section of a borehole;

z = longitudinal coordinate of cylindrical coordinates;

z_B = length of the test section;

$\kappa = c_p/c_v$ = ratio of specific heat at constant pressure to that at constant volume;

μ = viscosity of air;

ρ = density of air;

ρ_0 = density of air at atmospheric pressure;

Σ = summation over all elements; and

ϕ = porosity;

(Received November 27, 1992; revised May 13, 1993)